

Estimation of Maximum Tensile Stress on Rigid Pavement for Varying Surface Temperature

Deepa Das , Dibyendu Pal* 

Department of Civil Engineering, North Eastern Regional Institute of Science and Technology, Nirjuli-791109, Arunachal Pradesh, India

*Email: pal_here00@yahoo.co.in

Article Info

Received 18/06/2024

Revised 14/12/2024

Accepted 18/01/2025

Abstract

The load transfer ability of rigid pavement degrades over time due to repeated vehicular loads and environmental factors, such as temperature. The temperature disparity between a slab's upper and lower layers has more impact on the development of stresses on a rigid pavement. Failing of it occurs when the developed stresses exceed the critical stress. This work examines fluctuating surface temperatures' impact on the maximum tensile stress within a single slab system. The pavement was modeled and analyzed using the finite element software EverFE2.26. It was observed that varying surface temperature affects the maximum tensile stress. A regression model was developed to estimate the maximum tensile stress for any surface temperature (0°C-50°C), temperature differential, and other slab and axle parameters. The R^2 value of the regression model was obtained as 0.888. The regression model was validated with another set of maximum tensile stress data obtained from EverFE2.26. The model resulted in less than 10% difference. This model allows for directly estimating the maximum tensile stress in the rigid pavement, accommodating parameter changes. However, further model refinement may be carried out for multiple slabs.

Keywords: EverFE; Finite element analysis; Maximum tensile stress; Rigid pavement; Surface temperature

1. Introduction

Rigid pavements endure stresses due to the continuous action of vehicular loads and environmental factors. One of the ecological factors, i.e., the temperature in contact with the pavement, affects the performance of the pavement. Studies have shown that the load transfer stiffness of rigid pavement can degrade over time due to several factors, such as vehicular loads, aging of materials, and environmental conditions [1]. Climate change is expected to pose many challenges to the region's road planning, construction, and maintenance [2]. Frictional and warping stress are two different types of stress produced due to temperature variation. Warping stress occurs when there is a temperature disparity between a slab's upper and lower layers, and this temperature difference is denoted as temperature differential (ΔT). Frictional stress is generated by the resistance between the slab's underside and the soil beneath it. ΔT has more impact than any other slab parameters on stresses in the rigid pavement [3]. The temperature significantly affects the analysis and design of rigid pavement [4]. Linear ΔT cannot accurately predict the stresses. Nonlinear ΔT also causes displacement to the rigid pavement in the transverse direction. The ΔT and axle loads (P) combined cause critical stresses in the rigid pavement. Failure of rigid pavement is mainly when

the developed stress exceeds the necessary stress. Estimating these stresses for a given location is essential to prevent the rigid pavement from failing and make it more economical.

Many methods have been developed to estimate the stresses on rigid pavement. According to Westergaard, the maximum tensile stress (MTS) occurs in the pavement's edge location [5]. Westergaard developed the equations for rigid pavement stress analysis based on the plate theory. In this theory, a Winkler foundation was considered; a concrete slab was regarded as a thin elastic plate. The finite element approach was used to modify Westergaard's equation's limitation to achieve the MTS on the pavement's edge region [6]. A regression equation was developed to calculate the critical stresses on rigid pavement for different pavement parameters, P , and positive ΔT values [7]. A modified Bradbury's temperature stress coefficient was also suggested for calculating the curling stress on rigid pavement. Rigid pavements undergo analysis through plate theory instead of layer theory [8]. Plate theory simplifies layer theory by modeling the concrete slab as a medium-thick plate. This assumption posits that the plate is initially flat before loading and retains this flat configuration after loading.

In India, rigid pavements are developed according to the Indian Roads Congress (IRC) norms. IITRIGID software was used by IRC: 58-2002 to generate design charts using the concept proposed by Westergaard [9]. Design charts are generated from IITSLAB—II software using the concept of finite element analysis (FEA) in IRC: 58-2011 and IRC: 58-2015 [9].

Various numerical methods are available to analyze the problems based on engineering applications. Bezier multi-step method [10], finite difference method [11], and finite element method (FEM) [12],[13] are some examples. FEM is flexible in use and widely acceptable. It is widely seen that FEA is used to estimate stresses. Therefore, a detailed review in this context is carried out in the following sub-section.

In the last few years, the FEA concept has been used to solve various pavement problems [12],[13]. It is a method of decomposing a very complex problem into smaller, interrelated, and solvable parts. First, finite element programs in two dimensions (2-D) were created. Subsequently, three-dimensional (3-D) finite element programs were developed to overcome the constraints of the existing system. Some authors have analyzed rigid pavement using FEA-based software, such as ABAQUS [7], [14]-[17] ILLISLAB [18], KENSLAB [19], and EverFE [12], [20]-[25]. General-purpose finite element analysis (FEA) tools like ABAQUS and ANSYS excel at handling complex problems. However, effective use of these tools can be difficult, model creation can be time-consuming, 3-D simulations may require significant computation time, and extracting relevant results can be challenging [26]. Though these tools have several challenges, they can account for varying surface temperatures for calculating tensile stresses in rigid pavements. KENSLAB and ILLISLAB are finite element programs developed based on thin plate theory, i.e., the 2-D FEA program. Although ILLISLAB is widely used for modeling rigid pavements, it does not account for nonlinear thermal gradients within the pavement system [27]. Regarding simulating thermal loads, KENSLAB only supports a linear temperature distribution through the thickness of the material [26]. The range of applicability of 2-D FEMs is limited and is not capable of capturing detailed local responses, such as stress distributions near joints [12]. Three-dimensional (3-D) FEA programs were developed for rigid pavement to overcome limitations. EverFE is one of such 3-D finite element models.

EverFE provides greater flexibility by accommodating both linear and nonlinear temperature distributions. It allows up to four temperature change points along the thickness, resulting in linear, bilinear, or trilinear temperature profiles. Furthermore, in EverFE, the temperatures at these control points are specified as absolute values rather than relative differences. Different types of commonly used axle configurations have been included in EverFE, such as single-axle single-wheel, single-axle dual-wheel, tandem-axle single-wheel, and tandem-axle dual-wheel, which makes the model flexible to use.

EverFE was selected for this work to model the behavior of rigid pavements under wheel loads due to its specific advantages compared to other software. It is among the limited 3-D finite element tools designed explicitly for analyzing jointed concrete pavements. Work has shown that EverFE's

numerical results align well with field data, indicating its effectiveness in this type of analysis [27].

EverFE was chosen for this work to simulate rigid pavement performance. Numerous studies have demonstrated a high degree of agreement between EverFE numerical output and field data analytical results. EverFE, a 3-D FEA tool, was created by Professor William Davids to analyze deflection and stress in rigid pavement. The effect of various factors' response on the rigid pavement was analyzed using EverFE [12]. A realistic model was prepared in EverFE, which analyzed the model in three steps: pre-processing, processing, and post-processing. The program gave the stresses and deflection for a certain location within a limited time. Dowel bars and Tie bars come into effect for the pavement with multiple slabs. EverFE was used to analyze the impact of dowel misalignment, dowel locking, and looseness on the concrete pavement [20]. The effects of the transfer of loads at dowelled joints in the rigid pavement were also studied using EverFE [21]. The results showed that the pavements on soft soil experienced dowel looseness compared to those with stiff bases. No increase in damage was observed for an increase in dowel shears and dowel bearing stress.

In EverFE2.26 software, temperatures on the top and bottom of the slab can be incorporated to evaluate its effect on stresses. However, the same is not available in the IRC software. IRC: 58-2015 [9] does not consider the slab's actual surface temperature. It exclusively considers the temperature variations in the upper and lower layers of the slab. But EverFE considers the slab's real upper and bottom layer temperatures. The critical stresses differed in EverFE2.24 and IRC: 58-2015 [22]. The MTS obtained from IRC: 58-2015 was up to 42% less than those of IRC:58-2002, and the stresses obtained from EverFE2.26 were almost the same as IRC: 58-2002.

A similar comparison of stresses obtained from EverFE and Austroads was carried out [23]-[24]. EverFE overcomes some of Austroads' limitations. Hence, it was suggested that EverFE be used to analyze rigid pavements. The stresses due to future loadings in EverFE were analyzed, which were unattainable from Austroads [24]. A comparative study was conducted between the stresses obtained from EverFE2.26, ISLAB-2005, KENSLAB, IITRIGID, and Westergaard's equation [25]. The stresses resulting from the above software differed a lot from Westergaard's equation. Structural analysis of concrete pavement was carried out to evaluate the performance of KENSLAB and EverFE [26]. The key factors of modeling used in this work were element type, meshing, traffic load, temperature, boundary conditions, and contact conditions. EverFE software evaluated the critical stress on rigid pavement due to water in the expansive soil subgrade [28]. The edge stress of concrete pavement computed using ABAQUS was validated according to the solution of EverFE2.24 [14]. Hence, this work seeks to explore how surface temperature (ST) variations affect the MTS using FEA-based software EverFE2.26.

2. Materials and Methods

This work uses the FEA-based program EverFE2.26 to analyze the impact of variation in ST on MTS at the bottom surface of the rigid pavement for the single slab, tandem axle, and dual wheel conditions. The MTS is determined at the pavement's edge, which is the critical location. The next sub-section uses the finite element modeling concept to describe the model development in EverFE2.26.

This work considers three temperature zones: cold, moderate, and hot weather climatic conditions. The effect on MTS is computed due to variation in ST for different k, h, P, and ΔT (13°C, 17°C, and 21°C). Different slab parameters, such as size, h, P, k, etc., considered in this work align with the IRC: 58-2015, as shown in Table 1.

Table 1. Slab parameters, axle parameters, and temperature

Parameters	Value
Slab Dimension	4.5 m × 3.5 m
Slab thickness (h)	200 mm, 250 mm, 300 mm and 350 mm
Axle load (P)	160 kN, 200 kN, 240 kN, 320 kN, 400 kN and 480 kN
Modulus of Subgrade Reaction (k)	40 MPa/m, 80 MPa/m, 150 MPa/m and 300 MPa/m
Temperature differential (ΔT)	13°C, 17°C, 21°C
Axle and Wheel configuration	Tandem axle dual wheel
Modulus of elasticity of slab (E)	30,000 MPa
Poisson's ratio (μ)	0.15
Coefficient of thermal expansion (α)	$10 \times 10^{-6}/^{\circ}\text{C}$
Density of concrete	2400 kg/m ³

In this work, the sensitivity of E and α on the MTS for varying ST were checked. It was found that there was a negligible effect of E and α values at higher slab thickness. A minor variation was observed at a lower h (=200 mm) value. The E and μ vary depending on the cement concrete materials and their strength [9]. It is desirable to experimentally obtain these two parameters for the concrete mix and the materials used for construction. However, the same may not always be available at the design stage. Slight variation in E and μ values marginally affect the MTS in the pavement concrete [9]. Hence, an E value of 30,000 MPa and a corresponding μ value of 0.15 are used in this work. These values closely match the properties of the M40 grade concrete mix, which is standard for pavement applications. Standardizing these values, design codes, and guidelines ensures that pavement designs are safe and cost-effective, making E value 30,000 MPa a practical choice for most typical concrete pavements [9]. This value provides a representative

estimate that simplifies the design process, allowing consistency and ease of communication across various projects. The coefficient of thermal expansion (α) varies depending on the type of aggregate used in concrete. IRC:58-2015 [9] recommended a weighted value of $10 \times 10^{-6}/^{\circ}\text{C}$ for practical design purposes. Hence, the same was used in this work.

The following were the steps involved in the model's development:

- (i) Input slab properties, material properties, loading properties, ST = 0°C, modulus of subgrade reaction (k) = 40 MPa/m, slab thickness (h) = 200 mm, P = 160 kN, and $\Delta T = 13^{\circ}\text{C}$.
- (ii) Keeping all the parameters the same, ST increases from 0°C to 50°C with an interval of 10°C.
- (iii) For k = 80 MPa/m, 150 MPa/m, and 300 MPa/m, steps (i)-(ii) are repeated.
- (iv) Similarly, for h = 250 mm, 300 mm, and 350 mm, steps (i)-(iii) are repeated.
- (v) Further, for P = 200 kN, 240 kN, 320 kN, 400 kN, and 480 kN, steps (i)-(iv) are repeated.
- (vi) Finally, for $\Delta T = 17^{\circ}\text{C}$, and 21°C steps (i)-(v) are repeated.

A non-linearity can be attributed to material properties (use of tensionless dense liquid foundation, loosening of dowels, nonlinear aggregate interlocking models, or non-zero slab base transfer of shear) or slab base interface due to contact conditions [29]. None of these conditions were considered in this work, which makes the model linear.

The efficacy of the developed model was checked by comparing the MTS obtained from EverFE2.26 with the MTS obtained from the regression equation as recommended by IRC: 58-2015 [9]. The regression equations for different k values are available on page no. 74, Appendix V of IRC: 58-2015 [9]. Keeping all other parameters the same, the value of MTS for different h and k were obtained using the regression equations of IRC: 58-2015. At the same time, MTS for the same parameters were obtained from EverFE2.26.

A comparison of MTS for a single slab system (tandem axle dual wheel condition) and P = 200 kN obtained from EverFE2.26 and the regression equation given in IRC: 58-2015 is shown in Fig. 1. The legend k(E) and k(I) indicate the stress value obtained from EverFE2.26 and IRC: 58-2015 for that particular value of k, respectively. It is seen from Fig. 1 that IRC: 58-2015 underestimates the MTS, i.e., the MTS obtained from IRC equations is lower than the MTS obtained from EverFE2.26. However, the nature of the effect on MTS is the same due to the variation of h and k at constant ΔT and constant ST.

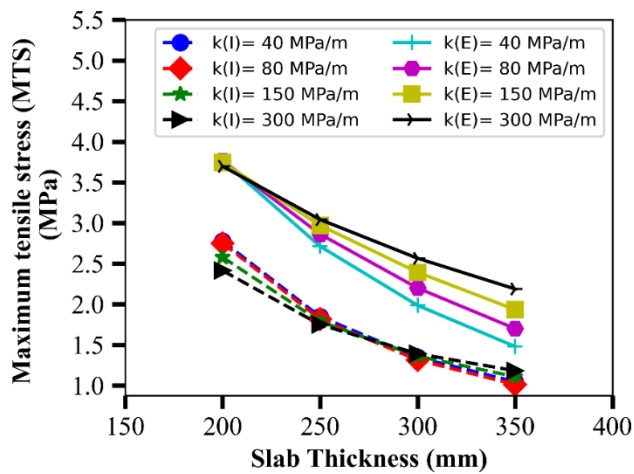


Figure 1. Comparison of MTS obtained from EverFE2.26 and IRC: 58-2015 [9]

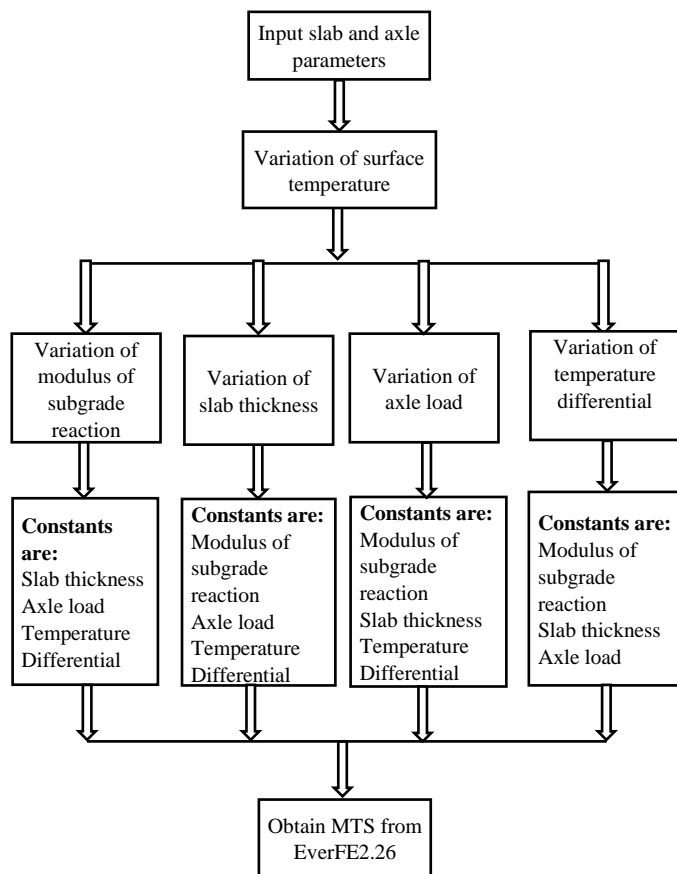


Figure 2. The flow of analysis of MTS with varying ST

Fig. 2 shows a flow chart of the analysis used to compute the MTS at the edge on the bottom surface of the pavement layer. The results and analysis of the computed MTS are illustrated in the following section. The MTS computed at 0°C ST is considered the base value. The change in stress in terms of percentage for increasing ST at an interval of 10°C up to 50°C is computed to check the effect of ST on MTS for different conditions.

3. Results and Discussion

3.1 Analysis of MTS

The following sub-sections analyze MTS to check its variation due to changes in different parameters such as k , h , P , and ΔT for varying ST.

3.1.1 Impact of 'k' on MTS

The variation of MTS for the change in ST and k is shown in Fig. 3. It is observed in Fig. 3(a) that for constant $P = 160$ kN, $h = 200$ mm, and $\Delta T = 13^\circ\text{C}$ the MTS increases on the increase in ST for all k . A similar nature can be seen in the case of $P = 320$ kN and 480 kN (Figs. 3(e) and 3(i)). However, at higher ST, the effect of k is more prominent. With $h = 250$ mm, k still affects MTS, but the MTS decreases at a low rate of decrement above an ST of 30°C (Fig. 3(b)). However, for $P = 320$ kN and 480 kN, MTS is almost flat to minimum positive above an ST of 30°C (Figs. 3(f) and 3(j)) for all k . With further increase in h (to 300 mm), for $P = 160$ kN, and $k = 300$ MPa/m, no effect of ST on MTS is observed above 10°C ST. MTS value between $k = 40$ MPa/m and 150 MPa/m decreases at a higher decrement rate after 20°C ST, as shown in Fig. 3(c). A similar trend is observed for all k values in the case of $P = 320$ kN and 480 kN above an ST of 30°C (Figs. 3(g) and 3(k)). For $h = 350$ mm, increasing ST has a minor or negligible effect on MTS for any k less than 300 MPa/m (Fig. 3(d)). For $P = 320$ kN, negligible impact of ST is observed up to an ST of 20°C. A slight increment in MTS is observed between 20°C and 30°C ST. Beyond an ST of 30°C, MTS slightly decreases for all k values (Fig. 3(h)). A similar trend is observed for $P = 480$ kN. A slight increment in MTS from 20°C to 40°C ST is observed, and beyond an ST of 40°C, MTS slightly decreases for all k values (Fig. 3(l)). Further analysis showed that for $P \geq 320$ kN, $h = 200$ mm, and $k \leq 300$ MPa/m, the MTS is also affected due to the increasing ST. However, the stress increment rate above 30°C ST was slower than that below 30°C ST. No further increase in MTS was observed for $h \geq 250$ mm and $k \leq 300$ MPa/m for an ST above 30°C. A similar trend was observed for $h = 300$ mm and 350 mm, and $k \leq 300$ MPa/m. A similar analysis was performed for $\Delta T = 17^\circ\text{C}$ and 21°C . It was observed that the ST affects MTS for all values of k at higher P . A negligible effect of the k value was seen on MTS for $h = 350$ mm.

3.1.2 Impact of 'h' on MTS

MTS obtained for $h = 200$ mm, 250 mm, 300 mm, and 350 mm are analyzed in this section to check the effect of slab thickness for varying ST. Fig. 4(a) shows the effect of ST on MTS for $k = 40$ MPa/m, $P = 160$ kN, $\Delta T = 13^\circ\text{C}$, and varying h . MTS increases with h up to 300 mm. However, for $h = 350$ mm, increasing ST does not affect the MTS. For $h = 200$ mm and 250 mm, negligible change in MTS may be seen beyond ST of 20°C. For $h = 300$ mm, the change in MTS increases to an ST of 20°C, whereas the same decreases beyond ST 20°C. Therefore, it can be said that for higher slab thickness (above 300 mm), increasing surface temperature may not increase the MTS. Parameters in Figs. 4(b & c) are the same as in Fig. 4(a), except $k = 80$ MPa/m and 150 MPa/m. Fig. 4(b & c) also shows a similar trend but with a slower rate of change of MTS.

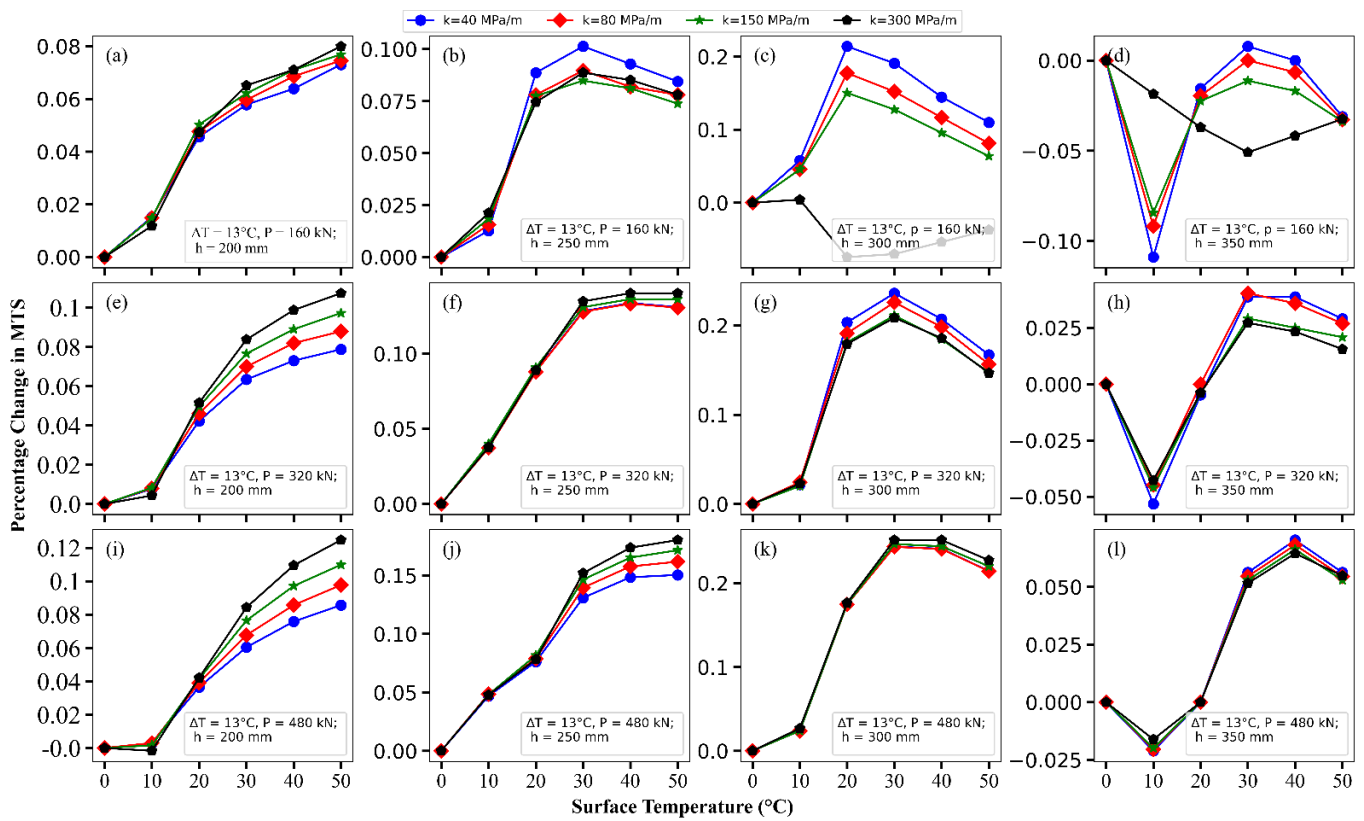


Figure 3. Effect of varying ST on MTS for different modulus of subgrade reaction (k)

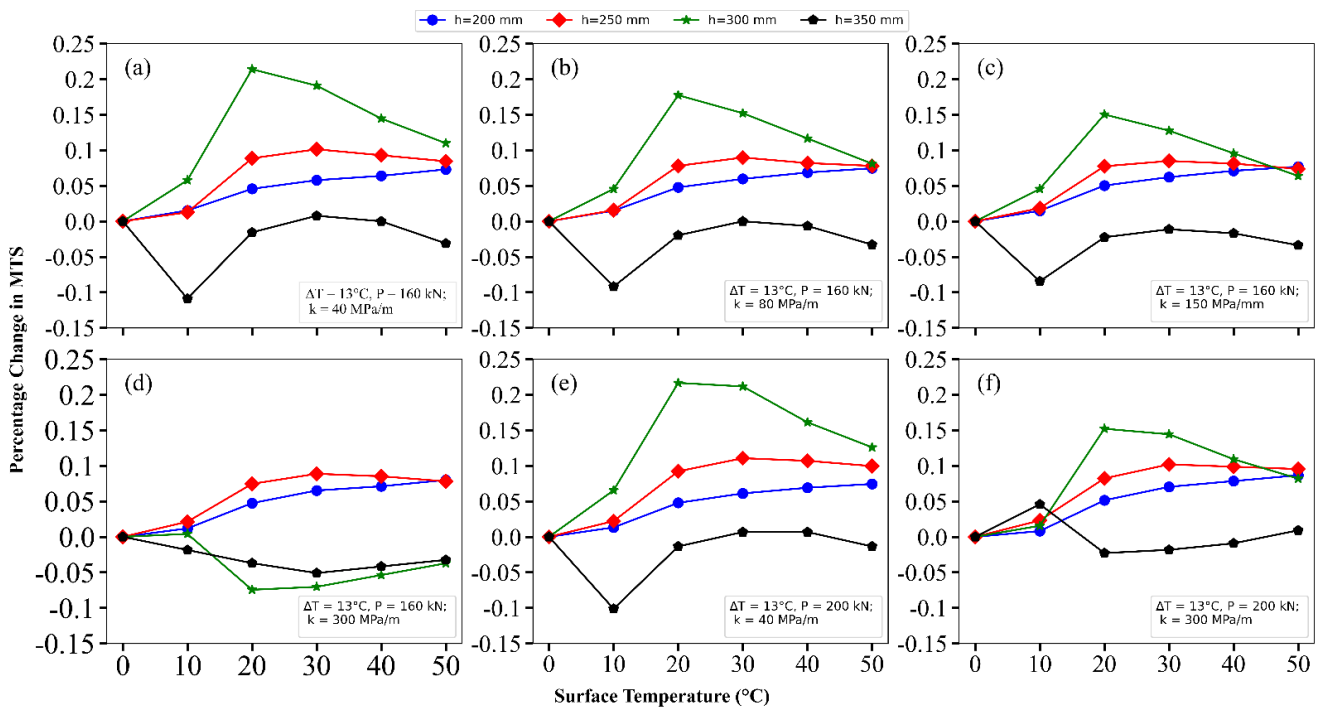


Figure 4. Effect of varying ST on MTS for different slab thickness (h)

MTS remains unaffected due to an increase in ST for $h \geq 300$ mm and $k \geq 300$ MPa/m (Fig. 4(d)). Fig. 4(d) also shows that $h \leq 250$ mm has minimal effect on the MTS as compared to lesser k values ($k < 300$ MPa/m). The impact of ST on MTS is shown in Figs. 4(e & f) for $P = 200$ kN, $k = 40$ MPa/m, and $P = 200$

kN, $k = 300$ MPa/m, respectively. It can be seen that similar to Figs. 4(a–d), in this case, $h > 300$ mm doesn't affect MTS (Fig. 4(e)). However, a negligible effect on MTS can be seen in the case of $k = 300$ MPa/m up to an ST of 20°C (Fig. 4(f)). It is seen from other cases, such as $P = 240$ kN, 320 kN, 400 kN, and 480

kN, that on increasing P, the effect on MTS is visible for higher h values. For example, in the case of Fig. 4(d), h = 300 mm has no effect, but Fig. 4(f) has shown an effect on MTS due to an increase in P.

Further analysis for $\Delta T = 17^\circ\text{C}$ and 21°C revealed that beyond 30°C ST, all values of h had an effect on the MTS for $P \geq 320$ kN and $P \geq 400$ kN, respectively. A slab thickness greater than 350 mm was observed to have a minor effect on MTS in all conditions.

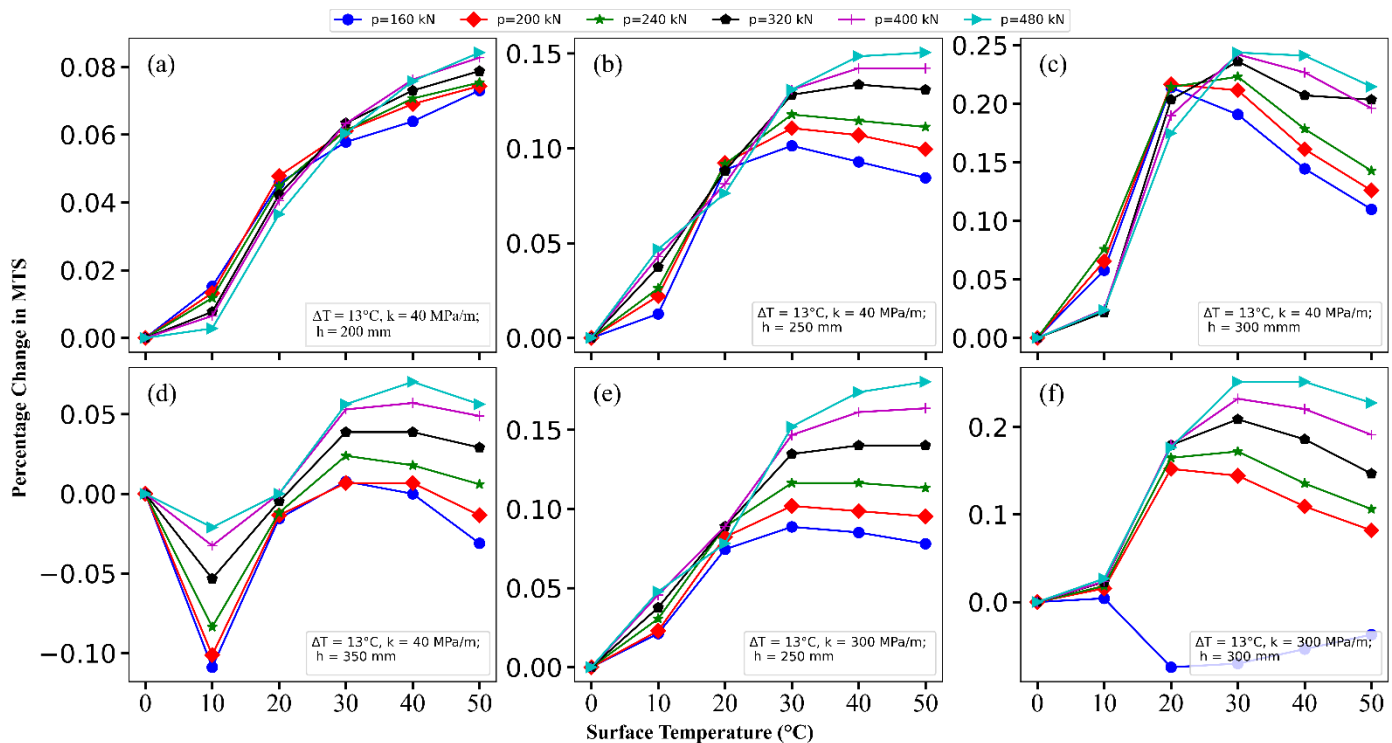


Figure 5. Effect of varying ST on MTS for different axle loads (P)

3.1.3 Impact of 'P' on MTS

This sub-section analyzes the effect of change in P on MTS for varying ST. Fig. 5(a) shows the effect of ST on MTS for $k = 40$ MPa/m, $\Delta T = 13^\circ\text{C}$, $h = 200$ mm, and varying P. Fig. 5(a) shows that all $P \geq 160$ kN affects the MTS. It can be seen in Fig. 5(a) that at lower ST, the effect on MTS due to higher P is less. However, beyond an ST of 30°C , the effect of higher P is more on MTS. It can be seen in Fig. 5(b) that in the case of $h = 250$ mm and same $k (= 40$ MPa/m), up to an ST of 30°C , MTS increased linearly on increasing ST. However, beyond an ST of 30°C , MTS is almost constant for higher P. As seen in Fig. 5(c), with the increase of h to 300 mm, the MTS increases to an ST of 20°C . Beyond an ST of 20°C , MTS starts declining at a lower decrement rate. For $h = 350$ mm, no effect is seen on the MTS up to 20°C of ST; beyond 20°C , minor effects can be seen (Fig. 5(d)). Fig. 5(e) shows MTS for $k = 300$ MPa/m and $h = 250$ mm. A similar trend as that of Fig. 5(b) is observed in Fig. 5(e). Fig. 5(f) shows MTS for $k = 300$ MPa/m and $h = 300$ mm. A similar trend is observed in Fig. 5(c), except that in the case of Fig. 5(f), MTS linearly increases up to an ST of 20°C . In the case of $k = 300$ MPa/m, $h = 300$ mm, $P = 160$ kN, increasing ST does not affect MTS. A similar analysis was performed for different P values. For higher P, all ΔT affects MTS for varying ST up to $h \leq 300$ mm. A minor effect of ΔT was seen for $h =$

350 mm for any P values. From the work, it was observed that for $\Delta T = 17^\circ\text{C}$ and 21°C , at $h = 200$ mm all P affected the MTS. But with the increase in h, the effect of the P on MTS starts decreasing on higher ST. With an increase in k and h, the effect of P on MTS was less. Therefore, it was concluded from this sub-section that the effect on MTS due to an increase in ST was more prominent in the case of higher P and higher ST for h up to 250 mm. Beyond $h = 250$ mm, an increase in ST had little effect in the case of lower P.

3.1.4 Impact of ' ΔT ' on MTS

This sub-section analyzes the effect of ST on MTS for variation in ΔT . It can be seen in Fig. 6(a) that for $P = 160$ kN, $h = 200$ mm, and $k = 40$ MPa/m, ΔT affects the MTS for an ST up to 50°C . Similar trends can be seen in Figs. 6(b) and 6(c) for $k = 80$ MPa/m and 150 MPa/m, respectively. Figs. 6(a-d) also depicts that lower ΔT has a higher effect on MTS due to increased ST. The $\Delta T \geq 21^\circ\text{C}$ has a minor or negligible effect on MTS due to varying ST for $k = 300$ MPa/m, as depicted in Fig. 6(d). Figs. 6(e & f) demonstrates that in the case of $h = 350$ mm and $k \geq 300$ MPa/m, ΔT has a negligible impact on MTS.

A similar analysis was performed for different P values. It was found that for higher P values, all ΔT values affect MTS for varying ST up to $h \leq 300$ mm. Minor or negligible effect of ΔT

was seen for $h = 350$ mm for any P values. The maximum MTS values were obtained at 50°C ST for $h = 200$ mm and 250 mm for all k values. For $h = 350$ mm and $k = 300$ MPa/m, the effect

of any ΔT on MTS was quite negligible compared to the other conditions.

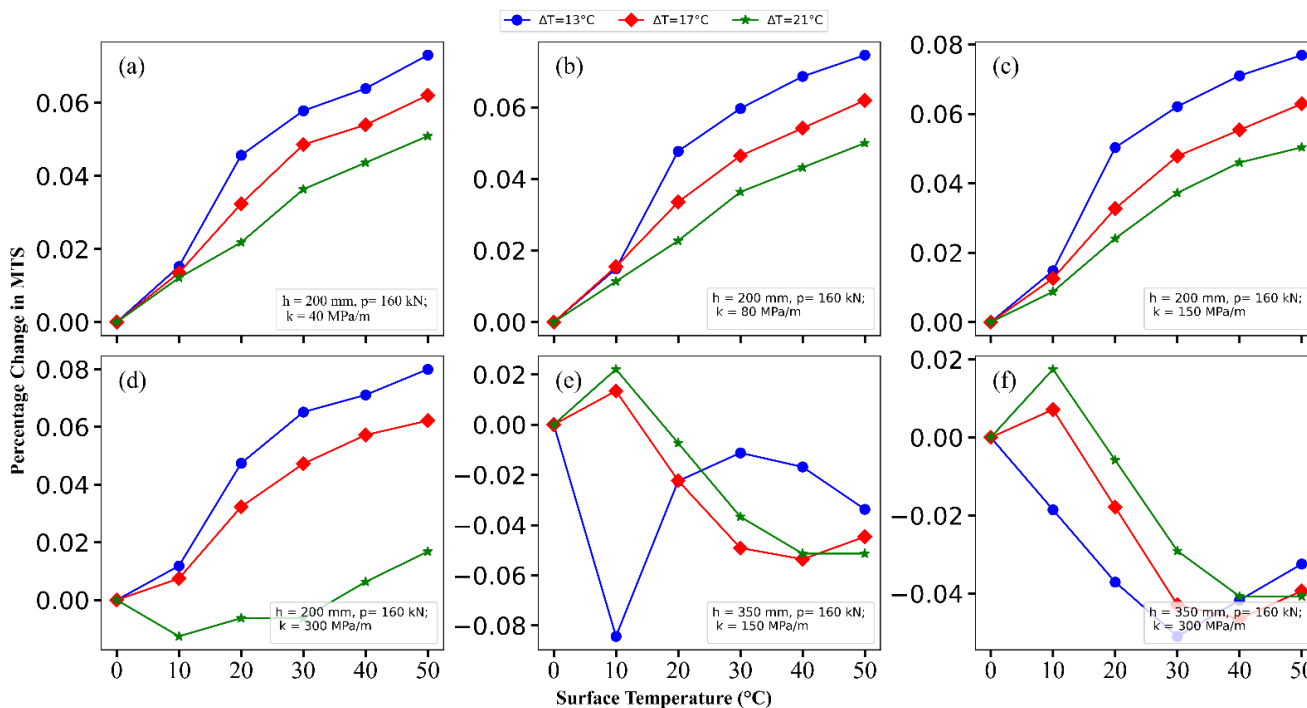


Figure 6. Effect of varying ST on MTS for different temperature differential (ΔT)

3.2 Regression Analysis

A regression analysis was performed on the results, i.e., MTS obtained for $P = 160$ kN, 200 kN, 240 kN, and 320 kN from EverFE2.26. A regression model for a single slab, tandem axle, and dual wheel condition was developed to consider the effects of ST on MTS. The equation functions developed were slab parameters (h, k, α, μ, E, l), $P, \Delta T$, and T_s . The empirical equation obtained for calculating the MTS from regression analysis is shown in “(1)”. Table 2 shows the variables that are parameters of the regression model “(1)”.

$$\sigma_T = 0.57 \times \frac{P}{h^2} + 18.22 \times \left(\frac{\alpha k l^2 \Delta T}{h}\right) - 0.91 \times \left(\frac{\alpha k l^2 T_s}{h}\right) + 0.52 \tag{1}$$

where,

σ_T = Maximum tensile stress due to the combined effect of wheel load and temperature differential (MPa)

P = Axle load (N)

h = Slab thickness of the concrete layer (mm)

k = Modulus of subgrade reaction (MPa/mm)

α = Coefficient of thermal expansion of concrete ($^\circ\text{C}$)

l = Radius of relative stiffness (mm)

$$l = \sqrt[4]{\frac{Eh^3}{12k(1-\mu^2)}}$$

T_s = Surface temperature of the concrete slab ($^\circ\text{C}$)

The regression statistics of the developed regression model “(1)” are shown in Table 2.

Table 2. Parameters of the regression model “(1)”

Variable	Coefficients	Standard Error	t Stat	p Value	Regression Statistics	Model Test
Constant	0.52	0.037	14.07	1.56×10^{-41}	Observations: 1152, RMSE: 0.354, R^2 : 0.888, SSE: 146.96	F statistic vs. zero model: 1166.21 p-value: 0
$\frac{P}{h^2}$	0.57	0.006	93.76	0.00		
$\left(\frac{\alpha k l^2 \Delta T}{h}\right)$	18.22	0.531	34.300	4.5×10^{-178}		
$\left(\frac{\alpha k l^2 T_s}{h}\right)$	-0.91	0.187	4.856	1.36×10^{-06}		

The MTS for different pavement parameters, P , ΔT , and ST of the concrete slab, can be estimated using “(1)”. A comparison between the MTS obtained from the “(1)” and EverFE2.26 for slab parameters $h = 200$ mm, $k = 40$ MPa/m, $E = 30,000$ MPa, $\mu = 0.1$, and $\alpha = 10 \times 10^{-6}/^\circ\text{C}$ are given in Table 3.

Table 3. Comparison of MTS in the concrete slab

Temperature	P (kN)	MTS (MPa) using		Differenc es (%)
		“(1)”	EverFE2.26	
$ST = 0^\circ\text{C}, \Delta T = 13^\circ\text{C}$	400	6.5588	6.1638	6.41
$ST = 50^\circ\text{C}, \Delta T = 13^\circ\text{C}$	400	6.4937	6.1689	5.27
$ST = 0^\circ\text{C}, \Delta T = 13^\circ\text{C}$	480	7.6988	7.1231	8.08
$ST = 50^\circ\text{C}, \Delta T = 13^\circ\text{C}$	480	7.6337	7.1291	7.08
$ST = 0^\circ\text{C}, \Delta T = 17^\circ\text{C}$	400	6.6631	6.5847	1.19
$ST = 50^\circ\text{C}, \Delta T = 17^\circ\text{C}$	400	6.5980	6.5894	0.13
$ST = 0^\circ\text{C}, \Delta T = 17^\circ\text{C}$	480	7.8031	7.5440	3.43
$ST = 50^\circ\text{C}, \Delta T = 17^\circ\text{C}$	480	7.7380	7.5495	2.50
$ST = 0^\circ\text{C}, \Delta T = 21^\circ\text{C}$	400	6.7673	7.0054	3.40
$ST = 50^\circ\text{C}, \Delta T = 21^\circ\text{C}$	400	6.7022	7.0098	4.39
$ST = 0^\circ\text{C}, \Delta T = 21^\circ\text{C}$	480	7.9073	7.9648	0.72
$ST = 50^\circ\text{C}, \Delta T = 21^\circ\text{C}$	480	7.8422	7.9699	1.60

The stress resulting from the proposed regression model closely aligns with the stress produced by EverFE2.26, exhibiting less than 10% disparity, as depicted in Table 3. The developed regression model for a single slab system with a tandem axle dual wheel on either side may be used to obtain the MTS without performing the rigorous finite element analysis.

4. Summary

This work uses FEA-based software EverFE2.26 to analyze and check the effect of ST on MTS for a single slab system of rigid pavement with tandem axle dual wheel conditions. Various values of k , h , P , and ΔT were considered in this work. The present work is summarized below:

- (i) Rigid pavement with various configurations was modeled using the FEA-based software EverFE2.26.
- (ii) Table 1 shows various parameters considered in this work. All these values were in line with IRC: 58-2015 [9]. ST between 0°C and 50°C was considered with an interval of 10°C .
- (iii) The efficacy of the developed rigid pavement model was examined by comparing the MTS obtained from EverFE2.26 and the regression equation of IRC: 58-2015 (Fig. 1). The nature of the effect in both cases was quite similar. However, IRC: 58-2015 underestimates the MTS.

- (iv) The effect of varying ST on MTS was observed for different k , h , P , and ΔT values. Based on the analysis performed using EverFE2.26, a flow chart was prepared.
- (v) The following were observed from the analysis of varying k to determine the MTS with variation in ST :

- All k values impacted MTS from $P = 200$ kN onwards for $\Delta T = 13^\circ\text{C}$, from $P = 240$ kN onwards for $\Delta T = 17^\circ\text{C}$, and from $P = 320$ kN onwards for $\Delta T = 21^\circ\text{C}$.
- A minor effect of k was seen on MTS in the case of $h = 350$ mm.
- The effect of k was prominent on MTS for higher ST .

- (vi) The effect of ST on MTS for variation of h (200 mm – 350 mm) for various conditions is summarized below:

- A negligible/minor $h = 350$ mm effect was seen on MTS for varying ST .
- Minor impact on MTS for varying ST for $h = 300$ mm and 350 mm was seen in the case of $k = 300$ MPa/m.

- (vii) The impact of P on MTS for varying ST is summarized below:

- All P values in this work impacted MTS for varying ST in the case of $k = 40$ MPa/m and 80 MPa/m.
- A minor effect of P was observed on MTS for varying ST for all cases when $h = 350$ mm.
- The impact of P on MTS for varying ST was reduced with an increase in ΔT values.

- (viii) The impact on MTS for different ΔT values is given below:

- All ΔT showed little effect on MTS for varying ST for $h = 350$ mm and $P \leq 240$ kN.
- For $P \geq 320$ kN, all ΔT affects the MTS for varying ST .
- Change in MTS for varying ST was less with an increase in ΔT .

- (ix) A regression model was developed to estimate MTS for varying ST and other parameters. The same can be seen in “(1)”.

- (x) The developed model's regression statistics were RMSE: 0.354, R^2 : 0.888, and SSE: 146.96 (Table 2).

- (xi) The MTS obtained from the developed regression model, and EverFE2.26 were compared (Table 3). The difference between them was less than 10%, which makes the developed regression model more feasible than performing rigorous FEA to obtain MTS.

5. Conclusions

This work investigated the MTS in rigid pavements under single slab, tandem axle, and dual wheel conditions, considering various slab parameters (h , k), P , ΔT , and ST . The

results showed that increasing ST significantly influenced MTS, especially for higher P and lower k values (40 MPa/m and 80 MPa/m). For thicker slabs (350 mm), the impact of varying ST on MTS was less. As ΔT increased, the effect of lower P values on MTS became negligible, with the most significant impact observed at higher P levels. The work also revealed that varying ST (0°C-50°C) affected MTS in non-reinforced rigid pavements. A regression model, incorporating ST and other variables, was developed to predict MTS. The R^2 of the regression model was achieved as 0.888. A comparison of MTS obtained from the developed regression model and EverFE2.26 was carried out. The difference between the MTS for both cases was less than 10%, suggesting the model's feasibility over more complex FEA methods. However, further validation and refinement using additional data for other conditions, multiple slabs, and axle configurations are recommended.

Acknowledgment

The authors wish to convey their sincere thanks to Professor William Davids, Civil and Environmental Engineering, University of Maine, United States, for granting access to EverFE2.26 software.

Conflict of interest

The authors declare that there are no conflicts of interest regarding the publication of this paper.

Author Contribution Statement

Deepa Das: Conceptualization, Methodology, Model development, Writing – original draft.

Dibyendu Pal: Supervision, Methodology, Writing - review and editing.

References

- [1] AASHTO, "Pavement management guide ."2nd ed., Washington, DC., 2012. Available: <https://store.transportation.org/Item/CollectionDetail?ID=117>
- [2] S. Serrao-Neumann et al., "Climate Change Impacts on Road Infrastructure Systems and Services in South East Queensland: Implications for Infrastructure Planning and Management," Griffith University, Gold Coast/QLD, Australia, 2011. [Online]. Available: http://soac.fbe.unsw.edu.au/2011/papers/SOAC2011_0144_final.pdf
- [3] D. M. Setiawan, "The role of temperature differential and subgrade quality on stress, curling, and deflection behavior of rigid pavement," *Journal of the Mechanical Behavior of Materials*, vol. 29, no. 1, pp. 94–105, Sep. 2020, doi: <https://doi.org/10.1515/jmbm-2020-0010>
- [4] I. E. Harik, P. Jianping, H. Southgate, and D. Allen, "Temperature Effects on Rigid Pavements," *J. Transp. Eng.*, vol. 120, no. 1, pp. 127–143, Jan. 1994, doi: [https://doi.org/10.1061/\(ASCE\)0733-947X\(1994\)120:1\(127\)](https://doi.org/10.1061/(ASCE)0733-947X(1994)120:1(127)).
- [5] P. Chakraborty and A. Das, "Principles of Transportation Engineering", 2nd ed. Delhi, India: PHI Learning Private Limited, 2017. Available: <https://www.phindia.com/Books/BookDetail/9788120353459/>
- [6] A. M. Ioannides and R. A. Salsilli-Murua, "Temperature Curling in Rigid Pavements: An Application of Dimensional Analysis," *Transportation Research Record: Journal of the Transportation Research Board*, vol. 1227, pp. 1–11, 1989. Available: <https://onlinepubs.trb.org/Onlinepubs/trr/1989/1227/1227-001.pdf>
- [7] S. R. Maitra, K. S. Reddy, and L. S. Ramachandra, "Estimation of Critical Stress in Jointed Concrete Pavement," *Procedia - Social and Behavioral Sciences*, vol. 104, pp. 208–217, Dec. 2013, doi: <https://doi.org/10.1016/j.sbspro.2013.11.113>.
- [8] M. R. Islam and R. A. Tarefder, "Pavement Design (Materials, Analysis, and Highways)." New York, United States of America: McGraw Hill, 2020. Available: <https://www.accessengineeringlibrary.com/content/book/9781260458916>
- [9] IRC: 58-2015, "Guidelines for the design of plain jointed rigid pavements for highways," New Delhi, India., 2015. Available: <https://www.irc.nic.in>.
- [10] H. Kabir and M. M. Aghdam, "A generalized 2D Bézier-based solution for stress analysis of notched epoxy resin plates reinforced with graphene nanoplatelets," *Thin-Walled Structures*, vol. 169, p. 108484, Dec. 2021, doi: <https://doi.org/10.1016/j.tws.2021.108484>.
- [11] Y. Wang, Y. Gu, and J. Liu, "A domain-decomposition generalized finite difference method for stress analysis in three-dimensional composite materials," *Applied Mathematics Letters*, vol. 104, p. 106226, Jun. 2020, doi: <https://doi.org/10.1016/j.aml.2020.106226>.
- [12] W. G. Davids, G. M. Turkiyyah, and J. P. Mahoney, "EverFE: Rigid Pavement Three-Dimensional Finite Element Analysis Tool," *Transportation Research Record*, vol. 1629, no. 1, pp. 41–49, Jan. 1998, doi: <https://doi.org/10.3141/1629-06>.
- [13] Z. A. Alkaissi and Y. M. Al-Badran, "Finite Element Modeling of Rutting for Flexible Pavement," *Journal of Engineering and Sustainable Development*, vol. 22, no. 3, pp. 1–13, May 2018. Available: <https://jeasd.uomustansiriyah.edu.iq/index.php/jeasd/article/view/314>
- [14] F. M. Hernández López, E. Tejada Piusseaut, E. A. Rodríguez Veliz, and C. A. Recarey Morfa, "3D-FE of jointed plain concrete pavement over continuum elastic foundation to obtain the edge stress," *Revista de la construcción. Journal of Construction*, vol. 19, no. 1, pp. 5–18, Apr. 2020, doi: <https://doi.org/10.7764/RDLC.19.1.5-18>.
- [15] M. T. Nguyen and N. T. V. Phan, "Effect of Dowel Bar Distance in Jointed Concrete Pavement Based on ABAQUS Program," in *ICSCA 2021*, vol. 268, J. N. Reddy, C. M. Wang, V. H. Luong, and A. T. Le, Eds., in *Lecture Notes in Civil Engineering*, vol. 268., Singapore: Springer Nature Singapore, 2023, pp. 955–963. doi: https://doi.org/10.1007/978-981-19-3303-5_87.
- [16] C. Liu, Z. Han, and C. Ding, "A Study of Mechanic Based on ABAQUS Software under Different Loads of Airport Pavement Crack," in *Proceedings of the 3rd International Conference on Information Technologies and Electrical Engineering*, Changde City Hunan China: ACM, Dec. 2020, pp. 439–445. doi: <https://doi.org/10.1145/3452940.3453024>.
- [17] G. A. Almarshadani and M. H. Al-Sherrawi, "Effect Change Concrete Slab Layer Thickness on Rigid Pavement," *Eng. Technol. Appl. Sci. Res.*, vol. 12, no. 6, pp. 9661–9664, Dec. 2022, doi: <https://doi.org/10.48084/etasr.5283>.
- [18] P.-S. Lin, Y.-T. Wu, T.-K. Huang, and C. H. Juang, "Equivalent Single-Axle Load Factor for Rigid Pavements," *J. Transp. Eng.*, vol. 122, no. 6, pp. 462–467, Nov. 1996, doi: [https://doi.org/10.1061/\(ASCE\)0733-947X\(1996\)122:6\(462\)](https://doi.org/10.1061/(ASCE)0733-947X(1996)122:6(462)).
- [19] H. T. Yu, L. Khazanovich, M. I. Darter, and A. Ardani, "Analysis of Concrete Pavement Responses to Temperature and Wheel Loads Measured from Instrumented Slabs," *Transportation Research Record*, vol. 1639, no. 1, pp. 94–101, Jan. 1998, doi: <https://doi.org/10.3141/1639-10>.
- [20] W. G. Davids, Z. Wang, G. Turkiyyah, J. P. Mahoney, and D. Bush, "Three-Dimensional Finite Element Analysis of Jointed Plain Concrete Pavement with EverFE2.2," *Transportation Research Record*, vol. 1853, no. 1, pp. 92–99, Jan. 2003, doi: <https://doi.org/10.3141/1853-11>.

- [21] W. G. Davids, "Effect of Dowel Looseness on Response of Jointed Concrete Pavements," *J. Transp. Eng.*, vol. 126, no. 1, pp. 50–57, Jan. 2000, doi: [https://doi.org/10.1061/\(ASCE\)0733-947X\(2000\)126:1\(50\)](https://doi.org/10.1061/(ASCE)0733-947X(2000)126:1(50)).
- [22] P. Aggarwal and S. K. Dwivedi, "Finite Element Analysis of Rigid Pavement Using Everfe2.24 & Comparison of Results with IRC58-2002 & IRC58-2015," *CiVEJ*, vol. 3, no. 1, pp. 15–19, Mar. 2016, doi: <https://doi.org/10.5121/civej.2016.3102>.
- [23] M. Y. Darestani, A. Nataatmadja, and D. P. Thambiratnam, "A Review of 2004 Austro roads Rigid Pavement Design," presented at the 22nd Australian Road Research Board Conference, Research into Practice, Canberra, Australia: CD Rom, Oct. 2006, pp. 1–17. Available: <https://search.worldcat.org/title/926649928>
- [24] J. P. Tobler, "Evaluation of EverFE Software for Designing Australian Concrete Pavements," Dissertation, The University of Southern Queensland, Faculty of Engineering and Surveying, Australia, 2015. [Online]. Available: <https://core.ac.uk/download/pdf/211499514.pdf>
- [25] P. G. Surve, J. Ghava, and U. J. Solanki, "Stress Comparison and Computation of Cumulative Fatigue Damage Factors by ITRIGID & Other Finite Element Programs," *Indian Highways*, vol. 49, no. 12, pp. 33–42, 2021. Available: <https://www.irc.nic.in//admnis/admin/showimg.aspx?ID=674>
- [26] H. Gu, X. Jiang, Z. Li, K. Yao, and Y. Qiu, "Comparisons of Two Typical Specialized Finite Element Programs for Mechanical Analysis of Cement Concrete Pavement," *Mathematical Problems in Engineering*, vol. 2019, pp. 1–11, Sep. 2019, doi: <https://doi.org/10.1155/2019/9178626>.
- [27] A. M. Shaban, A. Alsabbagh, S. Wtaife, and N. Suksawang, "Effect of Pavement Foundation Materials on Rigid Pavement Response," *IOP Conf. Ser.: Mater. Sci. Eng.*, vol. 671, no. 1, p. 012085, Jan. 2020, doi: <https://doi.org/10.1088/1757-899X/671/1/012085>.
- [28] W. Wibowo, A. Setyawan, Y. M. Purwana, and B. Setiawan, "Critical stress evaluation of rigid pavement due to the presence of water in expansive soil subgrade," *Eureka: PE*, no. 2, pp. 174–183, Mar. 2023, doi: <https://doi.org/10.21303/2461-4262.2023.002810>.
- [29] B. Davids, "EverFE Theory Manual. Department of Civil and Environmental Engineering," University of Maine, USA, 2003. Available: <https://civil.umaine.edu/everfe-2/>